

Improving Plant Disease Classification by Adaptive Minimal Ensembling

Antonio Bruno^{1†}, Davide Moroni^{1†}, Riccardo Dainelli², Leandro Rocchi², Silvia Morelli³, Emilio Ferrari³, Piero Toscano^{2†} and Massimo Martinelli^{1*†}

¹*Institute of Information Science and Technologies, National Research Council, Pisa, Italy*

²*Institute of BioEconomy, National Research Council, Firenze, Italy*

³*Barilla G. e R. Fratelli S.p.A., Parma, Italy*

Correspondence*:

Massimo Martinelli, Institute of Information Science and Technologies, National Research Council, Via Moruzzi 1, Pisa, Italy

massimo.martinelli@isti.cnr.it

† These authors have contributed equally to this work and share first authorship

2 ABSTRACT

3 A novel method for improving plant disease classification, a challenging and time-consuming
4 process, is proposed. First, using as baseline EfficientNet, a recent and advanced family of
5 architectures having an excellent accuracy/complexity trade-off, we have introduced, devised
6 and applied refined techniques based on transfer learning, regularization, stratification, weighted
7 metrics and advanced optimizers in order to achieve improved performance. Then, we go further
8 by introducing adaptive minimal ensembling, which is a unique input to the knowledge base of
9 the proposed solution. This represents a leap forward, since it allows improving the accuracy with
10 limited complexity using only two EfficientNet-b0 weak models, performing ensembling on feature
11 vectors by a trainable layer instead of classic aggregation on outputs. To our knowledge, such
12 an approach to ensembling has never been used before in literature. Our method was tested on
13 PlantVillage, a public reference dataset used for benchmarking models' performances for crop
14 disease diagnostic, considering both its original and augmented versions. We noticeably improved
15 the state of the art by achieving 100% accuracy in both the original and augmented datasets.
16 Results were obtained using PyTorch to train, test, and validate the models; reproducibility is
17 granted by providing exhaustive details, including hyperparameters used in the experimentation.
18 A Web interface is also made publicly available to test the proposed methods.

19 **Keywords:** Plant Diseases, Image Classification, Deep Learning, Adaptive Ensemble, Convolutional Neural Networks

1 INTRODUCTION

20 Early detection of plant stress is one of the most crucial practices in agriculture (Nagaraju and Chawla,
21 2020). Biotic stress in plants is caused by living organisms, specifically viruses, bacteria, fungi, nematodes,
22 insects, arachnids, and weeds, while abiotic stress is caused by environmental factors such as drought, heat,
23 cold, strong wind, flooding and nutrient deficiencies. In agriculture, both kinds of stress are a significant
24 cause of crop yield and quality loss leading to serious monetary harm when limits for the occurrence of
25 the stress are exceeded (Pantazi et al., 2020; Kashef, 2020). Although, over the years, genetics has made
26 available cultivars that are increasingly resistant to various types of stress, the issue of yield and quality

27 losses remains crucial at a global scale, especially since climate change leads to the co-occurrence of abiotic
28 and biotic stresses (Pandey et al., 2017). Even today, the majority of the inspections are done manually
29 by direct visual analysis, which may not make it easy to identify the disease and its type. Indeed, farmers
30 use their naked eyes for plant inspection, which needs constant observation, high skills and experience.
31 Some of them are supported by guidelines with basic concepts and aiding materials (pictures/notes to
32 identify symptoms and patterns of stress) that are relevant to distinguish between biotic and abiotic injuries
33 and determine the possible cause and solution to adopt. At other times, farmers might require technical
34 support to achieve a formal and complete diagnosis. In all these cases, the methodologies adopted are
35 time-consuming and expensive (Zhang et al., 2020), often not viable for large farms or not affordable for
36 small farms. Even the identification of weeds typology - broadleaf or grassy - is difficult in their early
37 stages (from germination to the development of the first four/six leaves), i.e. exactly when it would be
38 the most suitable time to counter them. This issue has increased the importance of automated infection
39 recognition and compelled researchers to devise methods or systems that can more accurately diagnose
40 the problem (Ma et al., 2017). In addition, the increased public concern about environmental conservation
41 coupled with the need for more efficient agriculture necessary to cope with the simultaneous increase in
42 population and reduction of available land) demands the introduction of new cost-effective and sustainable
43 methods and solutions to support farmers in their daily work. In this context, machine learning techniques
44 can finally trigger a revolution for the timely suppression of organisms harmful to plants and keep the use
45 of chemical treatment and other forms of intervention to economically and ecologically justified levels.

46 Computer vision-based methods are now being considered as a key enabler in this revolution. The
47 problem has a relatively long history, including several attempts based on the use of particular imaging
48 technologies such as thermal and stereo images (Prince et al., 2015), colour and depth images (Rousseau
49 et al., 2012) or even fluorescence imaging spectroscopy (Wetterich et al., 2013) coupled with *ad hoc*
50 image processing pipelines. Such advanced imaging modalities might provide very specific and accurate
51 analysis suitable for particular, especially high-revenue, crops in precision agriculture. However, standard
52 RGB images might be preferable for the broader adoption of vision-based methods for fighting plant
53 diseases even in low-resource and low-income areas of the world. Progresses in artificial intelligence and
54 their excellent classification capabilities on standard images have encouraged several research lines. For
55 instance, neural networks for plant disease classification have been used before (Huang, 2007) making
56 use in most of the cases of handcrafted features and conventional computer vision pipelines. Indeed,
57 independently of the application domain, typical computer vision techniques are composed of a pipeline of
58 phases that almost equally contribute to the quality of the final result. In the case of image classification,
59 in particular, the phases are (i) *preprocessing* for improving the image quality (e.g. denoising, colour
60 enhancement/balancing); *segmentation* for isolating the foreground from the background, to focus only
61 on the useful information; *feature extraction* for obtaining only the relevant information of the foreground
62 represented in a numeric vector (i.e. feature vector), mostly performed by a domain expert, and (iv)
63 *classification* for learning and performing a mapping between the input feature vector and output classes.

64 In the last years, the paradigm shift proposed by *deep learning* (LeCun et al., 2015), consisting in a way
65 to perform *representation learning* i.e. obtaining the data feature vector without involving a domain expert,
66 has allowed embedding and automatically performing all the phases described above.

67 Convolutional Neural Networks (CNNs or ConvNets) represent the Deep Learning in the scope of
68 Computer Vision and are state of the art (SOTA) in most tasks (Khan et al., 2020). Even if there are many
69 CNN archetypes, all of them are essentially composed by stacking a variable number of modules (that
70 usually share parameters to reduce complexity) consisting of the following layers applied sequentially:

- 71 • convolutional layers: they apply several adaptive filters to regions of the image obtaining their abstract
72 representation;
- 73 • pooling layers: they perform aggregations which have the twofold effect of summarising data, picking
74 only relevant elements, leading to dimensionality reduction;
- 75 • non-linear activation layers: they are used to obtain a more powerful and expressive representation,
76 reaching different levels of abstraction.

77 At the end of an architecture composed of the layers as mentioned above, one or more fully connected layers
78 can be stacked. This organization allows automatic preprocessing, segmentation and feature extraction
79 whilst classification/regression is feasible, putting a dedicated output module at the top of the architecture.
80 The very first conceived CNN was LeNet (LeCun et al., 1989) more than thirty years ago. Again, only in
81 the last ten years CNNs have been experiencing massive use and success, frequently improving the SOTA
82 on different tasks (Krizhevsky et al., 2012; Simonyan and Zisserman, 2015; He et al., 2016; Szegedy et al.,
83 2015; Howard et al., 2017; Hu et al., 2018; Wang et al., 2020).

84 CNNs have been adopted to tackle the problem of plant disease classifications. For instance, (Wang
85 et al., 2017) have applied transfer learning and fine-tuning of general-purpose architectures to provide
86 fine-grained disease severity classification in the case of the apple black rot images dataset, obtaining a best
87 90.16% performance using VGG16. Similarly, (Ferentinos, 2018) used AlexNet and GoogleNet, training
88 the models with the use of an open database of 87,848 images, containing 25 different plants in a set of 58
89 distinct classes of [*plant, disease*] pairs, achieving the best performance of 99.53%. For the training and
90 validation of deep learning paradigms, a number of datasets are available (Lu and Young, 2020). However,
91 all of them have some limitations e.g. in size, variety of plants, diseases coverage and extrinsic shooting
92 conditions (i.e. varying illumination and backgrounds). Among them, PlantVillage (Hughes and Salathe,
93 2015) has emerged as a *de facto* open reference datasets for plant disease classification and, as such, it
94 is considered has a benchmark in this paper, although it shares limitations of other datasets and, notably,
95 the presence of standard backgrounds instead of real-world ones. It should be noticed that a large-scale
96 benchmark dataset has been recently proposed (Liu et al., 2021), together with a new approach to disease
97 recognition. Still, such a dataset is not freely available and has not yet gained reference value. In general,
98 previous methods addressing the classification of PlantVillage images achieve good performance, however
99 they often do not sufficiently address the efficiency and complexity of the employed paradigms. Indeed, in
100 order to achieve more significant penetration and broader adoption of the methods, the proposed paradigms
101 should be capable of running on low resource hardware, especially on smartphones, even in the absence of
102 remote clouds.

103 In view of the above consideration, in this work we propose a new approach to plant disease classification
104 based on adaptive minimal ensembling. The main contribution is represented by a novel approach to
105 ensembling: different weak classifiers are trained and then combined to obtain a new combined classifier.
106 The novelties of the proposed approach are at least twofold: from one side, we propose a fully trainable
107 combination layer, granting end-to-end differentiability of the global architecture; then, in our approach, the
108 combination layer does not act on the output layers of the weak classifiers as in other classical approaches,
109 but the weak classifiers are truncated before. Namely, the final fully-connected layers of each weak classifier
110 are removed, and the combination happens directly at the *deep feature* level. In addition, such an approach
111 is brought into practice adopting a family of SOTA models, namely EfficientNet (Tan and Le, 2019),
112 known for their optimal complexity/performance trade-off, for each weak classifier. EfficientNet is refined
113 by applying advanced techniques on data and processing, significantly improving the classification task.
114 Namely, besides using ensembling, we perform transfer learning from ImageNet and introduce a novel

115 optimizer as well as a novel validation scheme together with other minor tricks. From an experimental
116 point of view, the paper provides an advance since it shows that adaptive minimal ensembling can be used
117 to reach top performance with a minimal computational burden compared to other promising schemes in
118 the literature. Indeed, improving state of the art, we achieve 100% accuracy on the PlantVillage dataset
119 using an ensembling of only two weak classifiers (and thus minimal) while at the same time requiring
120 less computational resources of the previous methodologies tested on PlantVillage dataset. As a final
121 contribution, carrying out the experiments both on the original PlantVillage dataset and on its augmented
122 version, we show that our method based on minimal ensembling is less sensitive to data augmentation with
123 respect to other methods reported in the literature, in which performance significantly drops when training
124 is not performed on the augmented dataset.

125 The paper is organized as follows. In Section 2 we describe our designing strategy in detail (including the
126 proposed models and the validation phases), focusing on novelty aspects of the solution. The experimental
127 setup is then introduced in Section 3 in which the number and typologies of experimental runs, including
128 hyperparameters and other details, are reported in order to guarantee reproducibility. In Section 4 the
129 obtained experimental results are reported and discussed, while Section 5 ends the paper with ideas for
130 future research.

2 MATERIALS AND METHODS

131 Among the pool of CNN architectures available in the SOTA for image classification, it was decided to use
132 the EfficientNet (Tan and Le, 2019) family as core component in this work. This was motivated by several
133 factors.

134 First, as the name suggests, EfficientNet improves the classification quality without having huge
135 complexity with respect to the models having similar classification performances. EfficientNet family
136 consists of 8 progressively improved versions (b0-b7) with limited complexity growth, all of them having
137 the inverted bottleneck MBConv (first introduced in MobileNetV2) as core module, which expands
138 and compresses channels reducing the complexity of convolution. The real novelty introduced is the
139 way EfficientNets perform scaling of the network to achieve optimal performances given a predefined
140 complexity. In the CNN literature, there are 3 main types of scaling as shown in Fig.1:

- 141 • *depth scaling*, which consists in increasing the number of layers in the CNN; it is the most popular
142 scaling method in the literature and allows to catch features at more levels of abstraction;
- 143 • *width scaling*, means increasing the number of convolutional kernels and parameters or channels,
144 giving the model the capability to represent different features at the same level;
- 145 • *input scaling*, means increasing the size/resolution of the input images, allowing to capture more
146 details.

147 Each of these scaling can be set manually or by a grid search, but there are two problems with the traditional
148 scaling method: first they increase the model complexity, usually exponentially, with tons of new parameters
149 to tune and, second, after a certain level, experiments show that scaling does not improve performances.
150 The scaling method introduced in the paper is named *compound scaling* and suggests that strategically
151 performing all scaling together delivers better results, because it is observed that they are dependent.
152 Intuitively, Tan and Le (2019) introduce a compound coefficient ϕ representing the amount of resources
153 available to the model and find the optimal scaling combination using that amount of resources following
154 the rules:

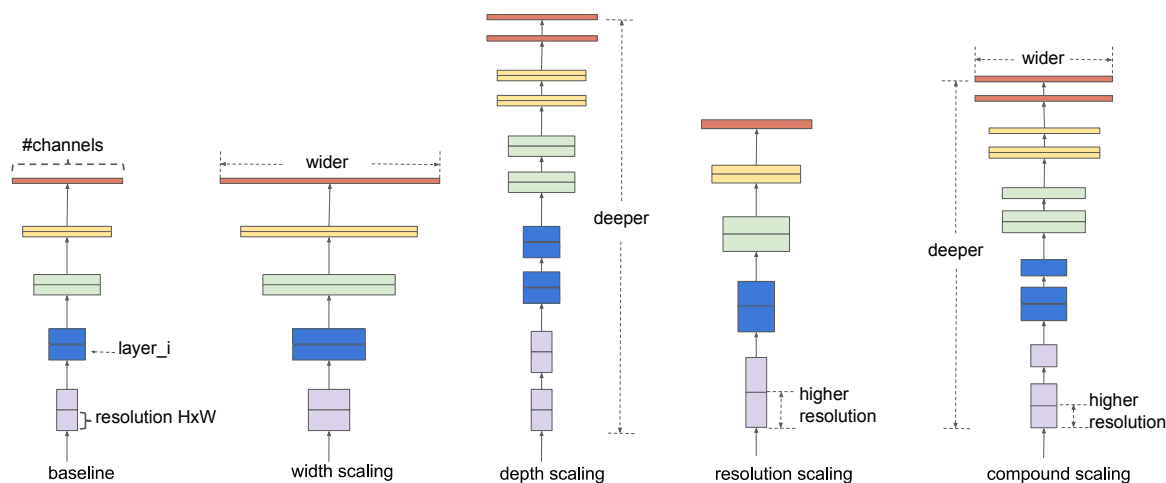


Figure 1. Example of scaling types, from left to right: a baseline network example, conventional scaling methods that only increase one network dimension (width, depth, resolution) and in the end the EfficientNet compound scaling method that uniformly scales all three dimensions with a fixed ratio. Image taken from the original paper (Tan and Le, 2019).

$$\begin{aligned}
 155 \quad & \text{depth: } d = \alpha^\phi \quad \text{width: } w = \beta^\phi \quad \text{resolution: } r = \gamma^\phi \\
 156 \quad & \text{such that } \alpha \cdot \beta \cdot \gamma^2 \approx 2 \quad \text{and} \quad \alpha \geq 1, \beta \geq 1, \gamma \geq 1
 \end{aligned}$$

157 In this way, the total complexity of the network is approximately proportional to 2^ϕ (see the original paper
 158 for more details). In the following sections, our strategy is illustrated, highlighting the differences from the
 159 previously cited works.

160 2.1 Input preprocessing

161 In many applications, the models are not fed directly with the images provided by the datasets, but
 162 images are preprocessed to improve the performances. In our study, since the image quality of the dataset
 163 of interest is already sufficient, we opted not to perform any image enhancement nor further augmentation
 164 because an augmented version of the dataset already exists.

165 The only preprocessing we applied is the normalization, in order to have all data described under the same
 166 distribution (pixel values in the $[0, 1]$ range and centred around the mean) which improves stability and
 167 convergence of the training.

168 2.2 Transfer learning

169 Transfer learning (Weiss et al., 2016) is the technique of taking knowledge gained while solving one
 170 problem, and applying it to a different but related problem. In this case, like the most cases for image
 171 classification, the stored knowledge is brought by pre-trained models from ImageNet (Deng et al., 2009)
 172 task, since it has more than 14 million images belonging to 1000 generic classes (including plants).

173 2.3 Avoid overfitting

174 In order to prevent overfitting (i.e. avoid the model being too specialized to the data from the training set
 175 with poor performances on *unknown* data), during training we use early stopping (i.e. training is interrupted
 176 after no improvements on the validation set after a certain number of epochs, called *patience*, is achieved)

177 and regularization (i.e. adding noise to the loss, usually proportional to the norm of the model parameter
178 vector, in order to keep parameters with low values).

179 2.4 Ensembling

180 Ensembling is the technique that combines several base models, called *weak*, in order to produce one
181 optimal model to achieve a better performance than any of the constituent models alone (Opitz and Maclin,
182 1999). The works (Dong et al., 2019; Sagi and Rokach, 2018) provide a comprehensive study on different
183 ensembling methods supported by empirical results. Instead of performing a sort of validation to obtain the
184 best combination of ensembling, we adopt the following heuristic choices:

- 185 • *ensemble main category*: due to its simplicity, we decided to use *bagging*, which consists in training
186 several independent weak models on different subsets of data. Since randomness (Ho, 1995) and
187 heterogeneity (Gashler et al., 2008) are known to lead to good quality ensembling, subsets are picked
188 totally random;
- 189 • *ensemble size*: the work in (Bonab and Can, 2016) provides the number of weak models to use for
190 obtaining the ideal ensemble model, however the work in (Bonab and Can, 2019) proves that a small
191 number of weak models is enough to achieve high performances with low complexity. We thus decided
192 to consider an ensembles size equal to 2 (i.e. the ensemble is composed of two weak models only,
193 being therefore minimal).
- 194 • *combination type*: the typical way of combining weak models is to perform voting/averaging as shown
195 in Fig.2 (predicting the output from all weak models and then picking the most frequent output/average
196 of outputs), respectively for classification/regression. However, in previous work, the ensemble is only
197 a static aggregator. In our method, we opted to perform an adaptive combination of the weak models; in
198 addition, instead of combining the outputs (Fig.3) of weak models, the features that the CNNs extract
199 from the input (Fig.4) are combined. In this way, the complexity of the ensemble is further reduced
200 without diminishing its power and expressiveness. Indeed the combination layer is of the same type of
201 the output layer as the weak models (i.e. Linear + LogSoftmax) and keeping both would introduce
202 an unnecessary redundancy. In particular, the mechanism adopted for the fusion of the ensemble is
203 performed first by concatenating the characteristics and then applying a linear transformation to match
204 the output size (i.e. we perform a kind of weighted sum on the concatenated features).
- 205 • *weak models training*: even if the work in (Sollich and Krogh, 1995) shows that overfitted weak models
206 might also lead to a good adaptive ensemble, we decided to train the weak models avoiding overfitting
207 to save precious training time and to have weak models of higher quality.

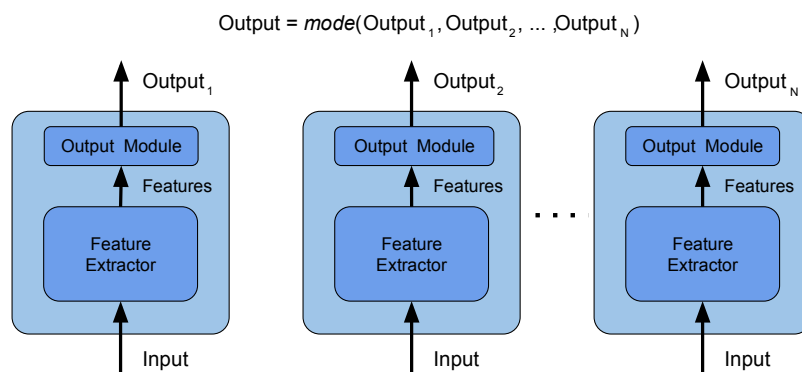


Figure 2. Ensemble by voting - the final label is obtained picking the most frequent label among the weak models. In this way, the weak models are independent and the ensemble is effective with a high number of heterogeneous weak models. Weak models are CNN architectures, since now represented by the sequence of Feature Extractor + Output module.

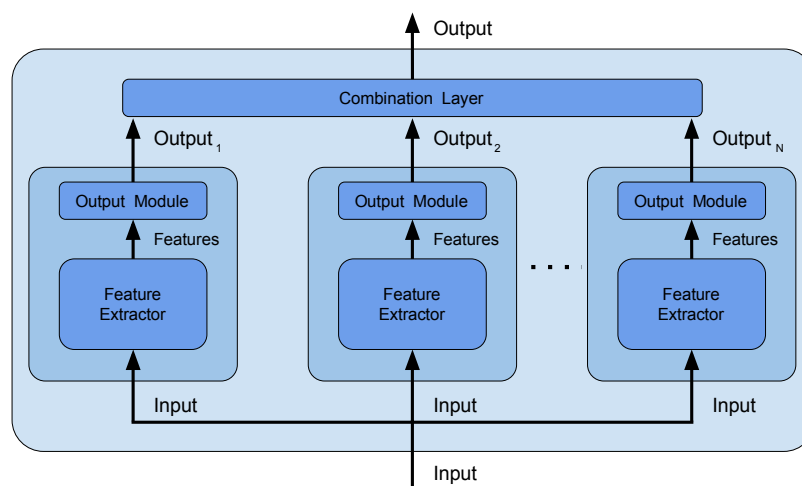


Figure 3. Ensemble by output combination - an additional combination layer is fed with the outputs of the weak models and combines them, in this way the weak models are no longer independent and the combination layer can be trained to better adapt to data.

208 2.5 Validation phases

209 The validation of each single model is divided into two main phases: first *end-to-end training* is performed
 210 and then followed by output module *fine-tuning*. For the first phase, transfer learning starting from the
 211 ImageNet pre-trained model is applied, introducing a new output module to adjust the output size from
 212 the 1000 classes in ImageNet task to the number of classes in the PlantVillage dataset. A training phase is
 213 performed using AdaBelief (Zhuang et al., 2020) optimizer which guarantees both fast convergence and
 214 generalization. The parameters used in AdaBelief are the default ones, i.e. learning rate equal to $5 \cdot 10^4$,
 215 betas (0.9, 0.999) and 10^{-16} , using weight decoupling without rectifying. After such training is concluded,
 216 the second phase starts: all the internal layers (i.e. the layers performing feature extraction) of the model
 217 obtained with the previous step are frozen and a new training by Stochastic Gradient Descent (SDG) with
 218 learning rate $3 \cdot 10^3$ and momentum 0.9 is performed. This leads to the fine-tuning of the output module
 219 of each classifier.

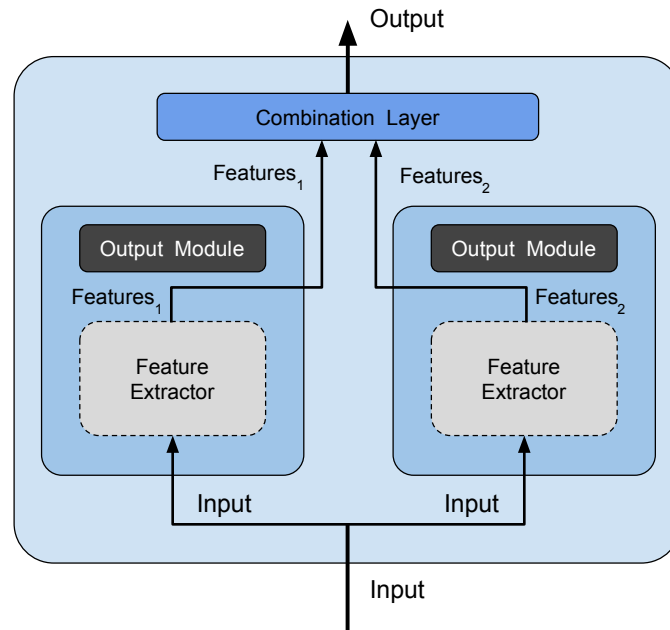


Figure 4. Our ensemble method - is an optimized version of the method shown in Fig.3 because we avoid redundancy and reduce complexity deleting the output module (dark gray filled) of weak models and feeding the combination layer directly with the features extracted by each weak model. Feature extraction modules (light gray filled with dashed borders) have the parameters frozen during ensemble training.

220 These steps conclude the validation phase for each single model. When going further to ensembling, each
 221 resulting single model is regarded as a weak model of a combined classifier and an additional dedicated
 222 pipeline is introduced for training the ensemble. First, the two best performing models are selected and
 223 truncated dropping their output module, which is replaced by a common combination layer. Then, ensemble
 224 fine-tuning (i.e. only the adaptive combination layer is trained) is performed using the same optimizer
 225 setting of the first validation phase. The reasons why we perform a dedicated pipeline for ensemble are
 226 described in Section 3.3.

227 2.6 The PlantVillage Dataset

228 The PlantVillage dataset (Hughes and Salathe, 2015) is a dataset for multiclass image classification tasks
 229 having 55,448 images (61,486 in its augmented version) divided into 39 classes representing background-
 230 only (out of domain images e.g. animals, buildings), healthy and diseased plants.

231 Table 1 shows that images span 14 plant species: Apple, Blueberry, Cherry, Corn, Grape, Orange, Peach,
 232 Bell Pepper, Potato, Raspberry, Soybean, Squash, Strawberry, Tomato and contains images of 17 fungal
 233 diseases, 4 bacterial diseases, 2 mold (Oomycete) diseases, 2 viral diseases and 1 disease caused by a mite
 234 (some examples are shown in Fig.5).

235

3 EXPERIMENTAL SETUP

236 In this section we describe the design choices justified by prior observations. All the reported experimnetal
 237 results were obtained using the PyTorch (Paszke et al., 2019) open-source machine learning framework.

238 A somewhat non-conventional training/validation/test splitting has been used in the experiments to
 239 reproduce the conditions closest to the work in (Ümit Atila et al., 2021) representing the SOTA for

Class Name	Class Frequency	Class Name	Class Frequency
Apple scab	630	Pepper healthy	1478
Apple black rot	621	Potato early blight	1000
Apple cedar apple rust	275	Potato healthy	1000
Apple healthy	1645	Potato late blight	152
Background without leaves	1143	Raspberry healthy	371
Blueberry healthy	1502	Soybean healthy	5090
Cherry powdery mildew	1052	Squash powdery mildew	1835
Cherry healthy	854	Strawberry healthy	1109
Corn gray leaf spot	513	Strawberry leaf scorch	456
Corn common rust	1192	Tomato bacterial spot	2127
Corn northern leaf blight	985	Tomato early blight	1000
Corn healthy	1162	Tomato healthy	1591
Grape black rot	1180	Tomato late blight	1909
Grape black measles	1383	Tomato leaf mold	952
Grape leaf blight	985	Tomato septoria leaf spot	1771
Grape healthy	1162	Tomato spider mites	1676
Orange haunglongbing	5507	Tomato target spot	1404
Peach bacterial spot	2297	Tomato mosaic virus	373
Peach healthy	360	Tomato yellow leaf curl virus	5357
Pepper bacterial spot	997		

Table 1. Class labels distribution of PlantVillage dataset. Some diseases are typical of particular plant phenotypes, there are also healthy leaf and background-only images. The frequency values refer to the standard dataset, while in the case of its augmented version only the classes with size less than 1000 were augmented to reach 1000 images (classes having more images are not modified).

240 PlantVillage while doing this work. More in detail, datasets have been splitted into training (90%),
 241 validation (7%) and test (3%). While obviously splits have the same sizes of previous papers, however, since
 242 the picks are random, the actual elements in each subset may vary. Moreover we performed stratification
 243 (i.e. preserving the classes ratio). Besides the non-conventional split, in the result and discussion section, a
 244 classic split is also considered to show the suitability of our strategy also in this case.

245 3.1 Loss and Metrics

246 **Training Loss:** due to the multiclass nature of the problem, the Cross-Entropy Loss (which exponentially
 247 penalizes differences between predicted and true values, expressed as probability of class belonging) is
 248 used. For this reason, the model output has size 39 (i.e. number of classes) and each element `output[i]`
 249 represents the probability that the input model belongs to class i .

250 **Validation and test metrics:** for the validation set evaluation, we decided to use the Weighted F1-score
 251 because this takes into account both correct and wrong predictions (true/false positive/negative) and
 252 weighting allows to manage any imbalance of the classes (more representative classes have a greater
 253 contribution). On the other hand, in order to compare our results ~~to make comparisons~~ with previous works,
 254 we used accuracy to evaluate the test set.

255 3.2 Hyperparameters

256 In order to save time, after an initial coarse search, we fixed some hyperparameters:

- 257 • early-stopping patience set at 10 because deep models have relatively fast convergence and they
 258 usually start overfitting after convergence, so there is no need to have much patience;



Figure 5. Some PlantVillage image examples. From top to bottom: 3 examples of background, 3 examples of healthy leaves and 3 examples of diseases.

- 259 • batch size set at 32 because it is the maximum size allowed on the GPUs we used to perform model
 260 training and lower values showed no improvement (and would make training slower). Stratification
 261 even inside the batches would have been desirable but this is possible only if the batch size is greater
 262 than the number of the classes, which is not our case;
- 263 • input image size fixed to 256 in order to preserve input image quality, larger size would ruin the
 264 images, lower size would reduce details;
- 265 • mean and standard deviation used for normalization:
- 266 $\mu = [0.4683, 0.5414, 0.4477]$ $\sigma = [0.2327, 0.2407, 0.2521]$ for augmented dataset
 267 $\mu = [0.4685, 0.5424, 0.4491]$ $\sigma = [0.2337, 0.2420, 0.2531]$ for dataset

268 Moreover, we observed that regularization was not needed during the end-to-end training phase, and, in
 269 some cases, it even led to worse results. Regularization is then used only in weak models (not used for
 270 ensemble) fine-tuning step, with following hyperparameters:

- 271 • regularization type: Lasso (L1), Ridge (L2)
 272 • regularization factor (λ): 0, 10^{-4} , $5 \cdot 10^{-4}$, 10^{-3} .

273 For each combination we used 3 different random seeds in order to obtain different model parameter
 274 initialization values, and different train/valid/test splits (useful to obtain random heterogeneous weak
 275 models for ensemble).

276 Considering each dataset, we had the following combinations:

- 277 • end-to-end phase: 8 (EfficientNet architectures ranging from b0 to b7) × 3 (random seeds) = 24
278 combinations;
- 279 • fine-tuning phase: 24(end-to-end phase results) × 2(regularization types) × 4(regularization factors)
280 = 192 combinations;

281 Since there are two datasets (standard, augmented), the total number of runs is equal to $2 \times (192) = 384$
282 excluding ensembling which is addressed in Sec. 3.3 below.

283 3.3 Adaptive minimal ensembling, improving performances with minimum complexity

284 The last experimental step is to evaluate the performances of ensembling. We opted to perform this step
285 using only EfficientNet-b0 as weak models and not the full family of weak models trained in Section 3.2.
286 This choice was motivated by two observations: first of all, the performances of all EfficientNet variants
287 after the end-to-end phase are very similar as we show in Table 2, but b0 variant is much simpler ($\approx 5M$
288 parameters vs $\approx 66.7M$ parameters of b7), so we decided to investigate on the simplest type of ensemble,
289 even in terms of number of parameters (and not just in terms of ensemble size using only 2 weak models).
290 Moreover we skipped the fine-tuning phase as it is used to optimize those parameters that are removed
291 during ensembling because they are redundant (notice however that we performed fine-tuning anyway
292 before, in order to collect experimental results to allow fair comparison and show the improvements
293 ensembling can offer over single models). For the ensemble phase we followed another validation scheme
294 that is, for each version of the dataset, the following:

- 295 1. five end-to-end training of EfficientNet-b0 with different initializations and data splits, results in Table
296 4;
- 297 2. no fine-tuning because the parameters involved in this phase would be removed during ensemble;
- 298 3. five fine-tuning of minimal ensemble composed of the two best weak models obtained at the point 1,
299 using different initializations and data splits.

300 In this way only 10 runs per dataset are performed, which are drastically fewer than 192 as described in
301 Section 3.2 and every run is much faster. All training runs had the same configuration: AdaBelief optimizers
302 with learning rate $5 \cdot 10^{-4}$, betas (0.9, 0.999), eps 10^{-16} , using weight decoupling without rectifying and
303 Weighted F1-score as validation metric.

304 It must be noted that using different seeds for each validation phase, both for end-to-end and for ensemble
305 fine-tuning, produces different dataset splits: this can be therefore viewed as a cross-validation and, by
306 averaging the values in Table 5 we obtain the same results proving that our solution is consistent.

4 RESULTS AND DISCUSSION

307 Every validation step results in incremental improvements: we discuss them one by one in the following.
308

309 **End-to-end phase:** as shown in Table 2 results are very similar, moreover considering both datasets there
310 is no architecture being always the best/worst in both cases. It is also important to say that already in this
311 phase we improved the SOTA: indeed, the best results until this work were obtained by Ümit Atilla et al.,
312 2021) with Validation Accuracy 97.62% and Test Accuracy 98.31% for the standard dataset, Validation
313 Accuracy 98.97% and Test Accuracy 99.38% for the augmented dataset. We relate this improvement to our

314 design choices: AdaBelief optimizer, performing stratification during dataset, using Weighted F1-score as
 315 validation metric and using normalization parameters taken from datasets instead of ImageNet defaults.

Model	Original			Augmented		
	Test	Valid	Train	Test	Valid	Train
EfficientNet-b0	99.6995	99.8454	99.9960	99.7832	99.8374	99.9982
EfficientNet-b1	99.5793	99.8454	100.000	99.8916	99.8141	99.9928
EfficientNet-b2	99.5192	99.7681	99.9140	99.7832	99.8374	99.9982
EfficientNet-b3	99.6394	99.8712	99.9860	99.8374	99.9303	99.9964
EfficientNet-b4	99.6995	99.8454	99.9980	99.5664	99.8606	99.9982
EfficientNet-b5	99.7596	99.7939	99.9920	99.9458	99.8606	99.9982
EfficientNet-b6	99.7596	99.8712	99.9880	99.7290	99.8141	99.9675
EfficientNet-b7	99.5192	99.8454	99.9960	99.8916	99.9303	99.9982

Table 2. Table with best Weighted F1-score results, for each EfficientNet variant, after first phase of validation (i.e. end-to-end training). The values of the best architectures are in bold.

316 **Fine-tuning phase:** as shown in Table 3, EfficientNet-b7 is the best architecture in both datasets. In
 317 major cases this phase led to no improvements, in a few cases it improves performances on training data
 318 without getting worse on validation/test (i.e. improvements without overfitting). The improvements are
 319 more noticeable for the standard dataset (because in the first phase results were lower) especially for b7
 320 variant obtaining improvements overall. We observed no differences among different regularization types
 321 and factors, but it was needed (because with $\lambda = 0$ we got no improvements).

Model	Original			Augmented		
	Test	Valid	Train	Test	Valid	Train
EfficientNet-b0	99.6995	99.8454	100.000	99.8916	99.8838	100.000
EfficientNet-b1	99.6995	99.8969	100.000	99.8916	99.8374	99.9982
EfficientNet-b2	99.5793	99.8712	100.000	99.7832	99.9303	99.9982
EfficientNet-b3	99.7596	99.8712	99.9900	99.8374	99.9303	99.9964
EfficientNet-b4	99.6995	99.8454	99.9980	99.5664	99.8606	99.9982
EfficientNet-b5	99.7596	99.7939	99.9920	99.9458	99.8606	99.9982
EfficientNet-b6	99.8197	99.8712	99.9900	99.7290	99.8141	99.9675
EfficientNet-b7	99.8197	99.8712	100.000	99.8916	99.9303	100.000

Table 3. Table with best Weighted F1-score results, for each EfficientNet variant, after second phase of validation (i.e. end-to-end training + fine-tuning). The values of the best architectures are in bold.

322 **Ensemble:** this phase gave a huge peak of improvement in both dataset, obtaining a perfect 100% accuracy
 323 on both versions of the dataset (Table 5) being much less complex (10M vs 66.7M total parameters of
 324 EfficientNet-b7 as shown in Table 7).

325
326

327 We lastly summarize the design choices and the improvements they led to.

328

329 **Transfer learning:** helped to speed up and optimize (because training from scratch done in the preliminary
 330 analysis always led to poor results) the end-to-end training phase;

Model	Original			Augmented		
	Test	Valid	Train	Test	Valid	Train
EfficientNet-b0	99.8197	99.9485	100.000	99.7832	100.000	100.000
EfficientNet-b0	99.8197	99.8969	100.000	99.6748	99.8838	100.000
EfficientNet-b0	99.7596	99.8454	100.000	99.8374	99.8374	99.9980
EfficientNet-b0	99.7596	99.7423	100.000	99.8374	99.6515	100.000
EfficientNet-b0	99.5793	99.9227	99.9960	99.7832	99.6747	100.000

Table 4. Table with Weighted F1-score of the models (best to worst) of the 5 end-to-end training runs using EfficientNet-b0 variants only that will be the weak models of the simplest ensemble.

Model	Original			Augmented		
	Test	Valid	Train	Test	Valid	Train
EfficientNet-b0 ensemble	100.000	100.000	100.000	100.000	100.000	100.000
EfficientNet-b0 ensemble	100.000	100.000	100.000	100.000	100.000	100.000
EfficientNet-b0 ensemble	100.000	100.000	100.000	100.000	100.000	100.000
EfficientNet-b0 ensemble	100.000	100.000	100.000	100.000	100.000	100.000
EfficientNet-b0 ensemble	100.000	100.000	99.9980	100.000	99.9768	100.000

Table 5. Table with the Weighted F1-score of the 5 ensemble runs (best to worst) composed of the two best EfficientNet-b0 variants.

Model	Dataset	
	Original	Augmented
Mohanty et al. (2016) (GoogleNet)	99.3500%	-
Too et al. (2019) (DenseNets-121)	99.7500%	-
Chen et al. (2020) (MobileNet-Beta)	99.8500%	-
Ümit Atila et al. (2021) (EfficientNet)	99.9100%	99.9700%
End-to-end (ours)	99.9729%	99.9904%
Fine-tuning (ours)	99.9856%	99.9919%
Minimal ensemble (ours)	100.000%	100.000%

Table 6. Table comparing accuracies (measured as correct prediction over the whole dataset) of the SOTA models on PlantVillage task. Since the end-to-end phase our work was shown to improve the SOTA.

331 **Adabelief optimizer:** allowed to reach lower minimal points due to its high convergence speed without
332 losing generalization power (previous SOTA work used Adam);

333 **Stratification and weighted F1-score:** reduced the problems due to high data imbalance, indeed in the
334 augmented dataset there is less imbalance and with the same condition there are better performances on it
335 (previous SOTA work used normal accuracy);

336 **Regularization:** harmful during end-to-end training but essential during fine-tuning, even if there is no
337 seeming difference among regularization types or factors (previous SOTA work does not seem to use
338 regularization);

339 **Ensembling:** using two weak models is enough to have meaningful improvements if the models are
340 heterogeneous enough (i.e. trained on different subset of data) even if they are very simple. This avoids
341 overfitting since training of weak models increased the base quality and reduced overall execution time.
342 Last but not least, performing ensembling on features instead of outputs further reduced the complexity
343 and deleted redundancies.

Model	Dataset	
	Original	Augmented
Mohanty et al. (2016) (GoogleNet)	≈ 7M	-
Too et al. (2019) (DenseNets-121)	≈ 7.9M	-
Chen et al. (2020) (MobileNet-Beta)	≈ 3.7M	-
Ümit Atila et al. (2021) (EfficientNet)	≈ 30.5M	≈ 19.5M
End-to-end (ours)	≈ 43.2M	≈ 66.7M
Fine-tuning (ours)	≈ 66.7M (100k)	≈ 66.7M (100k)
Minimal ensemble (ours)	≈ 10M (100k)	≈ 10M (100k)

Table 7. Table comparing complexity (measured as number of parameters) of the SOTA models on PlantVillage task. The minimal ensemble is the least complex because even if it has 10M parameters it can be considered as 5M because the weak models are independent and can be executed in parallel. Moreover, during training only the 100k parameters of the combination layers are trained.

344

345 Now we consider the comparison between our solution and the models representing the SOTA on the
 346 PlantVillage task over the years: Table 6 and Table 7 show that our design choices, different from previous
 347 works (i.e. AdeBelief optimizer, stratification, weighted-F1, regularization) improved performances if we
 348 consider single models. Our minimal ensemble method introduced in this work had a twofold improvement:
 349 perfect accuracy score without increasing model complexity. Moreover, the feature extractor modules
 350 are frozen making the real trainable parameters number very low even in the ensemble (100k trainable
 351 parameters over the 10M in total), and the execution of weak models can be performed in parallel since
 352 they are independent (so, the execution time for a 10M parameters ensemble is close to the execution time
 353 of a single 5M parameters model).

354 As said before, we performed a split to make a fair comparison with the SOTA (i.e. 90% train, 7% validation
 355 and 3% test). However, to prove its robustness, our solution has also been tested using a traditional 80/10/10
 356 split: few weak models were trained and then two best were used to run some ensemble fine-tuning, for
 357 each dataset version. The results in Table 8 prove that our solution is suitable also for traditional data splits.

Model	Original			Augmented		
	Test	Valid	Train	Test	Valid	Train
EfficientNet-b0 weak1	99.8738	99.8557	100.000	99.8536	99.8536	100.000
EfficientNet-b0 weak2	99.8377	99.9278	100.000	99.7886	99.9187	100.000
Ensemble (weak1 + weak2)	100.000	100.000	99.9864	100.000	100.000	100.000

Table 8. Table showing the accuracies of the two weak models and the fine-tuning ensembling them, using a traditional 80/10/10 split.

358 A Web application was also implemented to show the results, allowing to pick an image from the datasets
 359 and showing its classification and probabilities; this is publicly accessible at the following address:
 360 <http://plantvillage.isti.cnr.it:9090>.

5 CONCLUSION

361 Identifying plant diseases and devising optimal adaptive countermeasures can bring significant improvement
 362 in crop quality and yields. In this context, expert systems based on artificial intelligence can be a valid aid
 363 to farmers, yet there are still no operational services for most crops. This paper contributed to the creation

364 of artificial intelligence modules for plant disease classification with high accuracy and efficiency. Indeed,
365 it has been described how specific target design choices can lead to a relevant performance improvement
366 over an already top-rated solution without efficiency loss. The first improvement of the state of the art
367 was reached by using a different optimizer (i.e. Adabelief) in combination with techniques to deal with
368 unbalanced data (i.e. stratification and Weighted F1-score). A family of classifiers based on the EfficientNet
369 architecture has been proposed with similar accuracy but increasing complexity.

370 The second gain in performance was obtained by introducing a minimal adaptive ensemble model using
371 the combination of the features of two least complex weak models: while the number of total parameters
372 doubled with respect to the least complex model, perfect accuracy was achieved. To our knowledge, none
373 of the above mentioned techniques have been ever used before. Doubling the number of total parameters,
374 however, did not increase the total complexity for two reasons: first, only a tiny part of parameters is trained
375 during the ensemble training step (100k over 10M), and, second, the weak models can process input in
376 parallel (therefore the overall execution time is very close to the execution time of a single weak model).
377 In addition, by minimal ensembling, the performances gap between original and augmented datasets are
378 reduced; it could be argued that this type of ensembling can be helpful in cases where data balancing
379 and augmentation are not feasible or not convenient in terms of computational time/resources. These
380 perspectives will be studied in the future, considering other disparate domains and reference benchmarking
381 datasets. In particular, we are currently investigating the use of adaptive minimal ensembling and the
382 gains it is possible to achieve both in absolute average precision and in the ratio between precision and
383 complexity, towards a more sustainable use of artificial intelligence.

384 Regarding the precision agriculture domain, having achieved top performance on the *de facto* benchmarking
385 dataset, the research will pursue the possibility to provide operational service to farmers to identify and
386 recognize plant diseases. To this end, a participatory approach is being followed to gather a large dataset in
387 the specific domain of durum wheat crop culture from pictures taken in the field by farmers, also using
388 mobile devices. This initiative is leading to a realistic and more complex dataset to champion the methods
389 proposed in this paper.

CONFLICT OF INTEREST STATEMENT

390 The authors declare that they have no known competing financial interests or personal relationships that
391 could have appeared to influence the work reported in this paper.

AUTHOR CONTRIBUTIONS

392 All authors contributed to article that was coordinated by PT and MM. The data analysis and the experiments
393 were done by AB, DM and MM. The paper drafting was done by AB, DM, PT, MM. The manuscript was
394 written by AB, DM, MM, revised several times and approved by all the authors.

FUNDING

395 This work was partially supported by the *Barilla Agrosatplus* research project “DBA.AD001.034”.

ACKNOWLEDGMENTS

396 The authors wish to thank various colleagues for their contribution to this work: Simone Agostinelli,
397 Paolo La Cava, Rolando Maglione, Enrico Polverigiani, Gustavo Savino and Marco Silvestri for their very

398 valuable technical support, patient guidance, and useful critiques of this research work. The authors are also
399 particularly grateful to Ovidio Salvetti for his useful and constructive recommendations and enthusiastic
400 encouragement on this project.

DATA AVAILABILITY STATEMENT

401 The dataset analyzed for this study are referred in (Hughes et al., 2015) and can be found at the following
402 links: <https://github.com/spMohanty/PlantVillage-Dataset>
403 <https://data.mendeley.com/datasets/tywbtsjrjv/1>

REFERENCES

- 404 Bonab, H. and Can, F. (2019). Less is more: A comprehensive framework for the number of components
405 of ensemble classifiers. *IEEE Transactions on Neural Networks and Learning Systems* PP, 1–11.
406 doi:10.1109/TNNLS.2018.2886341
- 407 Bonab, H. R. and Can, F. (2016). A theoretical framework on the ideal number of classifiers for online
408 ensembles in data streams. In *Proceedings of the 25th ACM International on Conference on Information
409 and Knowledge Management* (New York, NY, USA: Association for Computing Machinery), CIKM '16,
410 2053–2056. doi:10.1145/2983323.2983907
- 411 Chen, J., fu Zhang, D., and Nanekaran, Y. A. (2020). Identifying plant diseases using deep transfer
412 learning and enhanced lightweight network. *Multimedia Tools and Applications*, 1 – 19
- 413 Deng, J., Dong, W., Socher, R., Li, L., Kai Li, and Li Fei-Fei (2009). Imagenet: A large-scale hierarchical
414 image database. In *2009 IEEE Conference on Computer Vision and Pattern Recognition*. 248–255.
415 doi:10.1109/CVPR.2009.5206848
- 416 Dong, X., Yu, Z., Cao, W., Shi, Y., and Ma, Q. (2019). A survey on ensemble learning. *Frontiers of
417 Computer Science* 14. doi:10.1007/s11704-019-8208-z
- 418 Ferentinos, K. P. (2018). Deep learning models for plant disease detection and diagnosis. *Computers and
419 Electronics in Agriculture* 145, 311–318
- 420 Gashler, M., Giraud-Carrier, C., and Martinez, T. (2008). Decision tree ensemble: Small heterogeneous is
421 better than large homogeneous. In *2008 Seventh International Conference on Machine Learning and
422 Applications*. 900–905. doi:10.1109/ICMLA.2008.154
- 423 He, K., Zhang, X., Ren, S., and Sun, J. (2016). Deep residual learning for image recognition. 770–778.
424 doi:10.1109/CVPR.2016.90
- 425 Ho, T. K. (1995). Random decision forests. In *Proceedings of the Third International Conference on
426 Document Analysis and Recognition (Volume 1) - Volume 1* (USA: IEEE Computer Society), ICDAR
427 '95, 278
- 428 Howard, A. G., Zhu, M., Chen, B., Kalenichenko, D., Wang, W., Weyand, T., et al. (2017) Mobilenets:
429 Efficient convolutional neural networks for mobile vision applications. *arXiv preprint arXiv:1704.04861*
- 430 Hu, J., Shen, L., and Sun, G. (2018). Squeeze-and-excitation networks. In *Proceedings of the IEEE
431 conference on computer vision and pattern recognition*. 7132–7141
- 432 Huang, K.-Y. (2007). Application of artificial neural network for detecting phalaenopsis seedling diseases
433 using color and texture features. *Computers and Electronics in agriculture* 57, 3–11
- 434 Hughes, D., Salathé, M., et al. (2015). An open access repository of images on plant health to enable the
435 development of mobile disease diagnostics. *arXiv preprint arXiv:1511.08060*

- 436 Hughes, D. P. and Salathe, M. (2015). An open access repository of images on plant health to enable
437 the development of mobile disease diagnostics through machine learning and crowdsourcing. *CoRR*
438 abs/1511.08060
- 439 Kashef, R. (2020). *Adopting Big Data Analysis in the Agricultural Sector: Financial and Societal Impacts*
440 (Singapore: Springer Singapore). 131–154. doi:10.1007/978-981-15-0663-5_7
- 441 Khan, A., Sohail, A., Zahoor, U., and Qureshi, A. S. (2020). A survey of the recent architectures
442 of deep convolutional neural networks. *Artificial Intelligence Review* 53, 5455–5516. doi:10.1007/
443 s10462-020-09825-6
- 444 Krizhevsky, A., Sutskever, I., and Hinton, G. E. (2012). Imagenet classification with deep convolutional
445 neural networks. *Communications of the ACM* 60, 84 – 90
- 446 LeCun, Y., Bengio, Y., and Hinton, G. (2015). Deep learning. *Nature* 521, 436–444
- 447 LeCun, Y., Boser, B., Denker, J. S., Henderson, D., Howard, R. E., Hubbard, W., et al. (1989).
448 Backpropagation applied to handwritten zip code recognition. *Neural Computation* 1, 541–551.
449 doi:10.1162/neco.1989.1.4.541
- 450 Liu, X., Min, W., Mei, S., Wang, L., and Jiang, S. (2021). Plant disease recognition: A large-scale
451 benchmark dataset and a visual region and loss reweighting approach. *IEEE Transactions on Image*
452 *Processing* 30, 2003–2015
- 453 Lu, Y. and Young, S. (2020). A survey of public datasets for computer vision tasks in precision agriculture.
454 *Computers and Electronics in Agriculture* 178, 105760
- 455 Ma, J., Du, K., Zhang, L., Zheng, F., Chu, J., and Sun, Z. (2017). A segmentation method for greenhouse
456 vegetable foliar disease spots images using color information and region growing. *Computers and*
457 *Electronics in Agriculture* 142, 110–117
- 458 Mohanty, S. P., Hughes, D. P., and Salathé, M. (2016). Using deep learning for image-based plant disease
459 detection. *Frontiers in Plant Science* 7, 1419. doi:10.3389/fpls.2016.01419
- 460 Nagaraju, M. and Chawla, P. (2020). Systematic review of deep learning techniques in plant disease
461 detection. *International Journal of System Assurance Engineering and Management* 11, 547–560
- 462 Opitz, D. W. and Maclin, R. (1999). Popular ensemble methods: An empirical study. *J. Artif. Intell. Res.*
463 11, 169–198. doi:10.1613/jair.614
- 464 Pandey, P., Irulappan, V., Bagavathiannan, M. V., and Senthil-Kumar, M. (2017). Impact of combined
465 abiotic and biotic stresses on plant growth and avenues for crop improvement by exploiting physio-
466 morphological traits. *Frontiers in plant science* 8, 537
- 467 Pantazi, X. E., Moshou, D., and Bochtis, D. (2020). Chapter 3 - utilization of multisensors and data
468 fusion in precision agriculture. In *Intelligent Data Mining and Fusion Systems in Agriculture*, eds.
469 X. E. Pantazi, D. Moshou, and D. Bochtis (Academic Press). 103–173. doi:https://doi.org/10.1016/
470 B978-0-12-814391-9.00003-0
- 471 Paszke, A., Gross, S., Massa, F., Lerer, A., Bradbury, J., Chanan, G., et al. (2019). Pytorch: An imperative
472 style, high-performance deep learning library. In *Advances in Neural Information Processing Systems*
473 32, eds. H. Wallach, H. Larochelle, A. Beygelzimer, F. d'Alché-Buc, E. Fox, and R. Garnett (Curran
474 Associates, Inc.). 8024–8035
- 475 Prince, G., Clarkson, J. P., Rajpoot, N. M., et al. (2015). Automatic detection of diseased tomato plants
476 using thermal and stereo visible light images. *PLoS One* 10, 1–20
- 477 Rousseau, D., Lucidarme, P., Bertheloot, J., Caffier, V., Morel, P., Chapeau-Blondeau, F., et al. (2012) On
478 the use of depth camera for 3d phenotyping of entire plants
- 479 Sagi, O. and Rokach, L. (2018). Ensemble learning: A survey. *Wiley Interdisciplinary Reviews: Data*
480 *Mining and Knowledge Discovery* 8, e1249. doi:10.1002/widm.1249

- 481 Simonyan, K. and Zisserman, A. (2015). Very deep convolutional networks for large-scale image
482 recognition. In *International Conference on Learning Representations*
- 483 Sollich, P. and Krogh, A. (1995). Learning with ensembles: How over-fitting can be useful. In *Proceedings*
484 *of the 8th International Conference on Neural Information Processing Systems* (Cambridge, MA, USA:
485 MIT Press), NIPS'95, 190–196
- 486 Szegedy, C., Liu, W., Jia, Y., Sermanet, P., Reed, S., Anguelov, D., et al. (2015). Going deeper with
487 convolutions. In *Computer Vision and Pattern Recognition (CVPR)*
- 488 Tan, M. and Le, Q. (2019). EfficientNet: Rethinking model scaling for convolutional neural networks.
489 In *Proceedings of the 36th International Conference on Machine Learning*, eds. K. Chaudhuri and
490 R. Salakhutdinov (PMLR), vol. 97 of *Proceedings of Machine Learning Research*, 6105–6114
- 491 Too, E. C., Yujian, L., Njuki, S., and Yingchun, L. (2019). A comparative study of fine-tuning deep
492 learning models for plant disease identification. *Computers and Electronics in Agriculture* 161, 272–279.
493 doi:<https://doi.org/10.1016/j.compag.2018.03.032>. BigData and DSS in Agriculture
- 494 Wang, G., Sun, Y., and Wang, J. (2017). Automatic image-based plant disease severity estimation using
495 deep learning. *Computational intelligence and neuroscience* 2017
- 496 Wang, J., Sun, K., Cheng, T., Jiang, B., Deng, C., Zhao, Y., et al. (2020). Deep high-resolution
497 representation learning for visual recognition. *IEEE transactions on pattern analysis and machine*
498 *intelligence*
- 499 Weiss, K., Khoshgoftaar, T., and Wang, D. (2016). A survey of transfer learning. *Journal of Big Data* 3.
500 doi:10.1186/s40537-016-0043-6
- 501 Wetterich, C. B., Kumar, R., Sankaran, S., Junior, J. B., Ehsani, R., and Marcassa, L. G. (2013). A
502 comparative study on application of computer vision and fluorescence imaging spectroscopy for detection
503 of citrus huanglongbing disease in usa and brazil. In *Laser Science* (Optical Society of America),
504 JW3A–26
- 505 Zhang, N., Yang, G., Pan, Y., Yang, X., Chen, L., and Zhao, C. (2020). A review of advanced technologies
506 and development for hyperspectral-based plant disease detection in the past three decades. *Remote*
507 *Sensing* 12. doi:10.3390/rs12193188
- 508 Zhuang, J., Tang, T., Ding, Y., Tatikonda, S., Dvornek, N., Papademetris, X., et al. (2020). Adabelief
509 optimizer: Adapting stepsizes by the belief in observed gradients. *Conference on Neural Information*
510 *Processing Systems*
- 511 Ümit Atila, Uçar, M., Akyol, K., and Uçar, E. (2021). Plant leaf disease classification using efficientnet deep
512 learning model. *Ecological Informatics* 61, 101182. doi:<https://doi.org/10.1016/j.ecoinf.2020.101182>